

The first analytical expression to estimate photometric redshifts suggested by a machine

A. Krone-Martins¹, E.E.O. Ishida^{2,3}, R. S. de Souza^{4,5}

¹*SIM, Faculdade de Ciências, Universidade de Lisboa, Ed. C8, Campo Grande, 1749-016, Lisboa, Portugal*

²*IAG, Universidade de São Paulo, Rua do Matão 1226, 05508-900, São Paulo, SP, Brazil*

³*Max-Planck-Institut für Astrophysik, Karl-Schwarzschild-Str. 1, D-85748 Garching, Germany*

⁴*Korea Astronomy & Space Science Institute, Daedeokdae-ro 776, 305-348 Daejeon, Korea*

⁵*MTA Eötvös University, EIRSA "Lendulet" Astrophysics Research Group, Budapest 1117, Hungary*

28 February 2022

ABSTRACT

We report the first analytical expression purely constructed by a machine to determine photometric redshifts (z_{phot}) of galaxies. A simple and reliable functional form is derived using 41, 214 galaxies from the Sloan Digital Sky Survey Data Release 10 (SDSS-DR10) spectroscopic sample. The method automatically dropped the u and z bands, relying only on g , r and i for the final solution. Applying this expression to other 1, 417, 181 SDSS-DR10 galaxies, with measured spectroscopic redshifts (z_{spec}), we achieved a mean $\langle (z_{\text{phot}} - z_{\text{spec}})/(1 + z_{\text{spec}}) \rangle \lesssim 0.0086$ and a scatter $\sigma_{(z_{\text{phot}} - z_{\text{spec}})/(1 + z_{\text{spec}})} \lesssim 0.045$ when averaged up to $z \lesssim 1.0$. The method was also applied to the PHAT0 dataset, confirming the competitiveness of our results when faced with other methods from the literature. This is the first use of symbolic regression in cosmology, representing a leap forward in astronomy-data-mining connection.

1 INTRODUCTION

A novel methodology was recently proposed to automatically search for underlying analytical laws in data (Schmidt & Lipson 2009). Its importance has been highlighted into astronomy by Graham et al. (2013), and this letter is the first attempt to use it in a cosmological context. We applied the aforementioned method to derive an analytic expression for photometric redshift (photo- z) determination from Sloan Digital Sky Survey 10th data release spectroscopic sample of galaxies (SDSS-DR10, Ahn et al. 2013). Our goal here is to demonstrate the potential of machine proposed analytical relations in providing simple and reliable photo- z .

Due to the variety of spectra occurring in nature (as there are several types of galaxies, of different ages, metallicities, star-forming histories, merging histories, etc.), the unicity of photometric redshift estimates is not assured for any sample. Nevertheless, the large amount of data expected to be observed by surveys like the Large Synoptic Survey Telescope¹ (LSST Science Collaboration et al. 2009), EUCLID² (Refregier et al. 2010) or Wide-Field Survey Infrared Telescope³ (Green et al. 2012) makes it infeasible to obtain spectroscopic redshifts for all their objects with the current and likely near future technology. Therefore making photo- z is the only viable solution for estimating redshifts in such large scale.

Photo- z methods have been widely used in fields as diverse as gravitational lensing (e.g., Mandelbaum et al. 2008; Zitron et al. 2011; Nusser et al. 2013), baryon acoustic oscillations (e.g., Nishizawa et al. 2013), quasars (e.g., Richards et al. 2009), luminous red galaxies (LRGs, de Simoni et al. 2013) and supernovae

(e.g., Kessler et al. 2010). At the same time, numerous efforts to accurately determine photo- z were reported (for a glimpse on the diversity of existent methods, see Abdalla et al. 2011; Hildebrandt et al. 2010; Zheng & Zhang 2012, and references therein). To deepen our understanding of the differences between photo- z techniques, Abdalla et al. (2011) compared results from six methods applied to LRGs. They show 1- σ scatters between 0.057 and 0.097 when averaged over the considered redshift range ($0.3 \leq z \leq 0.8$), systematically presenting poor accuracy at low ($z \leq 0.4$) and high ($z \geq 0.7$) redshifts. More recently, Hildebrandt et al. (2010) presented a wider comparison enclosing 16 different methods. The methods perform better in simulated than real data, with empirical codes showing smaller biases than template-fitting ones.

The existing approaches are usually divided in two classes: empirical (e.g. Connolly et al. 1995; Collister & Lahav 2004; Wadadekar 2005; Miles et al. 2007; O’Mill et al. 2011; Reis et al. 2012; Carrasco Kind & Brunner 2013) and template-fitting-based methods (e.g., Benítez 2000; Bolzonella et al. 2000; Ilbert et al. 2006). The former uses magnitudes and/or colours of a spectroscopically measured sample for training the method, which is then applied to the photometric sample. The latter, try to find spectral template and redshift which best fit the photometric observations using a library of well know observational or synthetic spectra.

The main advantage of the approach adopted in this letter is that without any *a priori* physical information nor *ad hoc* functional form, it empirically derives analytical expressions from the data. Besides that, the error propagation from the observables can be straightforwardly performed into the redshift estimate. Also, due to its analytic nature, the outcomes are more tractable, and thus interpretable, than the outcomes of other methods, such as neural-networks or support vector machines, for instance. Finally, the resulting expressions are promptly portable, and might be even in-

¹ <http://www.lsst.org/lsst/>

² <http://sci.esa.int/euclid/>

³ <http://wfirst.gsfc.nasa.gov/>

2 Analytical photo-z determination

corporated on-the-fly via *structured query language* (SQL) when retrieving catalogue data, for instance.

The outline of this letter is as follows. In Section 2, we give a broad picture of the methodology followed in this letter. Then, section 3, provides an overview of the adopted dataset. Afterwards, we present our results and compare with the recent literature in in Section 4. Finally, conclusions are presented in Section 5.

2 METHODOLOGY

The ultimate goal of symbolic regression-based techniques is to find a functional form that explains hidden associations in datasets, while optimizing a given error metric (e.g., Schmidt & Lipson 2009). This is fundamentally distinct from linear and non-linear regression methods that fit parameters for an *a priori* analytical expression. In symbolic regression, the machine searches the best expression and the optimal coefficients simultaneously.

We used the software EUREQA⁴ (Schmidt & Lipson 2009) to test the application of symbolic regression for photo-z determination. It allows the user to choose atomic function blocks (basic mathematical operations, exponentials, logarithms, boolean operators, trigonometric functions, etc.). Then, EUREQA scans through the data and a variety of combinations between the atomic function blocks are evolved through genetic programming (Koza 1992), optimizing conciseness and accuracy. Lastly, the outcome functions are ordered according to their complexity and quality of the fit.

The application of EUREQA to our problem follows a straightforward approach. First, a subset of galaxies with measured spectroscopic redshifts is used to derive an analytical expression that optimally predicts the redshift from the magnitude and colour data. In other words, an expression whose evaluation minimizes the mean absolute error when compared to the data. To seek simplicity while keeping accuracy, we only allowed the use of simple mathematical operations (+, −, *, /). Afterwards, the obtained expression is applied to a larger sample of galaxies with spectroscopic measurements, to perform a strict validation of the expression's predictive capability against real spectroscopic redshifts.

3 DATA

The data adopted in this work was selected from the SDSS-DR10 spectroscopic sample. This includes hundreds of thousands of new galaxies and quasars spectra from the Baryon Oscillation Spectroscopic Survey⁵ (BOSS) in addition to all imaging and spectra from prior SDSS data releases.

From this dataset, we selected all objects with spectroscopic measurements (table `SpecObj`) classified as galaxies (flag `SpecObj.class = 'GALAXY'`) and whose spectra were free from known problems (flag `SpecObj.zWarning = 0`). Moreover, only sources with clean photometric measurements (flag `PhotoObj.CLEAN = 1`) were accepted. The SQL query used in SDSS CasJobs⁶ service was

```
SELECT s.specObjID, g.u, g.g, g.r, g.i, g.z,
       s.z AS redshift
INTO mydb.specObjAllz_cleanphoto
```

⁴ <http://www.nutonian.com/products/eureqa/>

⁵ <http://www.sdss3.org/surveys/boos.php>

⁶ <http://skyserver.sdss3.org/casjobs/>

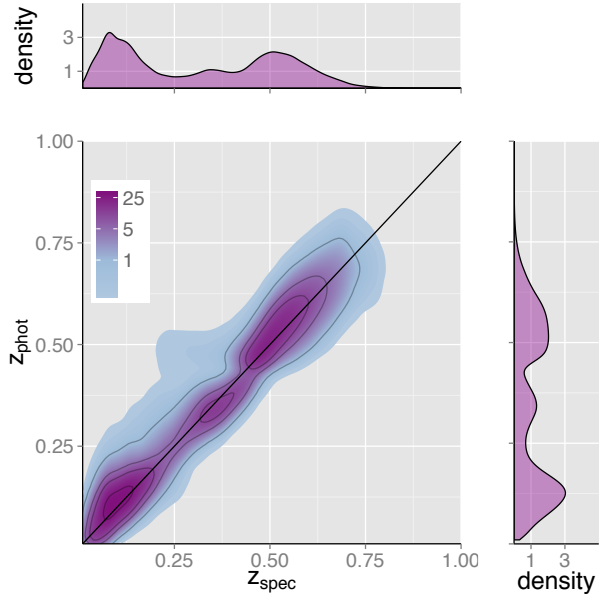


Figure 1. Kernel density distribution of photometric (z_{phot}) versus spectroscopic (z_{spec}) redshifts for more than one million SDSS-DR10 galaxies. The colour scale is logarithm, so a difference of one is equivalent to a density variation by a factor of e . Distributions for z_{spec} and z_{phot} redshifts are shown on the top and right panels.

```
FROM SpecObj AS s JOIN Galaxy AS g
ON s.specobjid = g.specobjid, PhotoObj
WHERE class = 'GALAXY' AND zWarning = 0
AND g.objId = PhotoObj.ObjID
AND PhotoObj.CLEAN=1
```

where `s.specObjID` is the object identification in the spectral tables, and `g.u, g.g, g.r, g.i, g.z, s.z` represent the SDSS' *ugriz* model magnitudes and measured spectroscopic redshift, respectively. This resulted into a dataset containing 1,458,404 objects, from which we retained only galaxies with $z_{\text{spec}} < 1.0$. Additionally, all possible color combinations based on the available photometric bands were computed.

We divided the data into two subsets, one for deriving the analytic expression and another for validation and error assessment. To mitigate biases created by unbalanced data, we randomly selected 5,000 galaxies per redshift bin (width $\Delta z_{\text{spec}} = 0.1$) up to $z_{\text{spec}} = 0.8$. For $0.8 \leq z_{\text{spec}} < 1.0$, half of all available objects in each redshift bin were used for deriving the expression. This comprises a total of 41,214 galaxies that were used for searching the expression. Then, the accuracy (systematic errors) and precision (random errors) of this expression was assessed based on other 1,417,181 objects. We only considered objects with $z_{\text{spec}} > 0$.

Finally, we did not apply any cuts in magnitude, quality of spectroscopic redshift measurement nor galaxy types. This ensures that our results are not biased towards high signal to noise data, a particular galaxy type nor optimal observation conditions in comparison with the SDSS-DR10 spectroscopic sample.

4 RESULTS

Adding the ingredients described so far, the optimal functional form suggested by EUREQA to the adopted dataset is

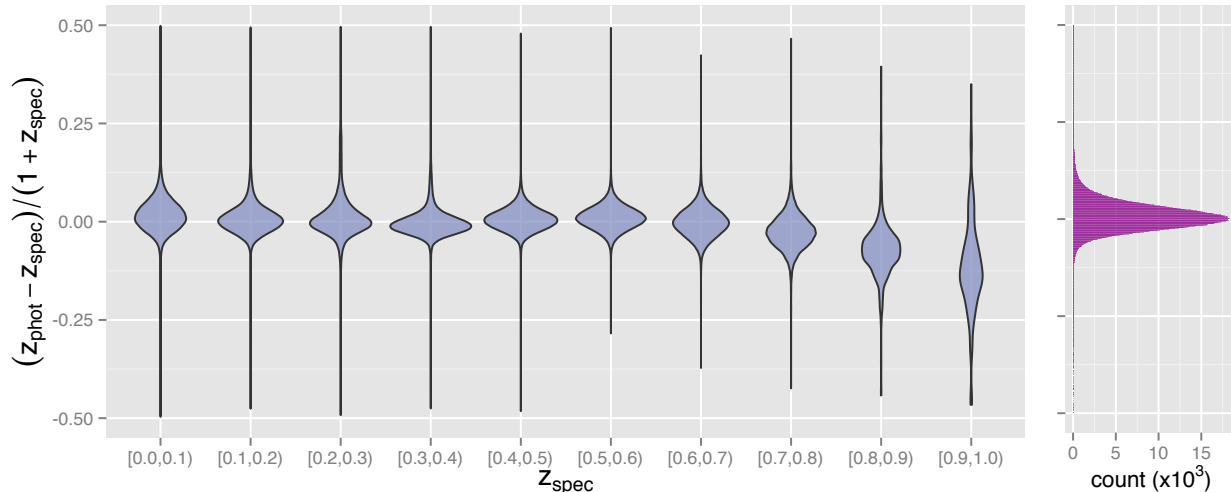


Figure 2. Left panel shows the photometric redshift error distributions estimated from Eq. 1, in redshift bins of width $\Delta z_{\text{spec}} = 0.1$. Right panel displays the error distribution for more than one million galaxies in SDSS-DR10 as a histogram with bins of width $\Delta((z_{\text{phot}} - z_{\text{spec}})/(1 + z_{\text{spec}})) = 0.001$.

$$z_{\text{phot}} = \frac{0.4436r - 8.261}{24.4 + (g - r)^2(g - i)^2(r - i)^2 - g + 0.5152(r - i)} \quad (1)$$

This represents a rather simple empirical relation between photometric measurements and redshifts of galaxies calibrated for the SDSS-DR10 spectroscopic sample⁷. Given its analytical nature, Eq. 1 allows a straightforward error propagation from the uncertainties in the measured magnitudes to the final photometric redshift. Note the missing u and z bands in the former equation. Such behavior was observed in several equations constructed by EUREQA, suggesting that a competitive performance might be reached using only three SDSS photometric bands⁸.

Interestingly, the two SDSS filters kept out of the derived equation are those which do not bracket the main spectral feature for imprinting redshift signature in photometry, for the redshift range considered in this work: the $\sim 4000\text{\AA}$ break. This does not mean that these filters carry null information. Instead, it only highlights that the bulk of information relevant to photometric redshift determination relies on the other filters. Due to a compromise between error and complexity during the optimization procedure, only the most relevant filters survive to the output equations. Moreover, the expressions assembled by EUREQA are not simply high order polynomials with additional terms, but more intricate combinations of magnitudes in different filters. Accordingly, expressions with more terms are not necessarily expected to improve redshift estimates, as additional terms might even introduce degeneracies.

To test the performance of Eq. (1), we applied it to the photometric data of 1,417,181 galaxies. Figure 1 summarizes our results, showing a comparison between z_{spec} and z_{phot} . One can promptly notice that z_{spec} is well recovered by z_{phot} with reasonable accuracy. Furthermore, a reasonable match between z_{spec}

and z_{phot} distributions can be observed (upper and right panels, respectively). This indicates that Eq. (1) recovers the underlying redshift distribution over a significant fraction of the explored redshift range.

Left panel of figure 2 shows the probability distribution functions (PDF) of $(z_{\text{phot}} - z_{\text{spec}})/(1 + z_{\text{spec}})$ in each redshift bin (width $\Delta z_{\text{spec}} = 0.1$) for $0 \leq z_{\text{spec}} < 1.0$, represented as violin plots. Each “violin” centre represents the median of the distribution, while the shape, its the mirrored PDF. The drop in medians at high redshifts ($z_{\text{spec}} \gtrsim 0.7$) indicates that z_{phot} systematically underestimates z_{spec} at this range. This might be caused by poor statistics: in the full dataset, at $z_{\text{spec}} \geq 0.8$ there are only 2,428 objects, while for $z_{\text{spec}} \geq 0.7$ there are 25,439. This underweights the contribution of high- z objects to the construction of Eq. (1). Accordingly, for bins with equally balanced number of galaxies ($z_{\text{spec}} \leq 0.7$), no obvious systematic effects are seen.

Right panel of figure 2 shows a histogram of $(z_{\text{phot}} - z_{\text{spec}})/(1 + z_{\text{spec}})$, with bins of 0.001, forming a nearly perfect normal error distribution. As the mean and standard deviation are known to be sensitive to outliers, we removed the extreme tails of z_{phot} distribution prior to computing them (117 events, or less than 0.008 per cent of the sample). This rejection is performed directly in the z_{phot} distribution without any prior knowledge about z_{spec} . The mean is $\langle (z_{\text{phot}} - z_{\text{spec}})/(1 + z_{\text{spec}}) \rangle \approx 0.0086$, while the scatter is $\sigma_{(z_{\text{phot}} - z_{\text{spec}})/(1 + z_{\text{spec}})} \approx 0.0449$.⁹ Albeit using a different dataset, Hildebrandt et al. (2010) obtained similar values ($0.005 \leq |(z_{\text{phot}} - z_{\text{spec}})/(1 + z_{\text{spec}})| \leq 0.039$ and $0.034 \leq \sigma_{(z_{\text{phot}} - z_{\text{spec}})/(1 + z_{\text{spec}})} \leq 0.076$). Nevertheless, given the different adopted datasets, we refrain from performing a direct comparison with our results. Notwithstanding, these figures suggest that equations derived by EUREQA might be competitive against more elaborated methods.

Using a homogeneous sample of LRGs, Abdalla et al. (2011) tested six different methods, reporting $0.0014 \leq |(z_{\text{phot}} - z_{\text{spec}})| \leq$

⁷ We stress that this expression was calibrated for the SDSS-DR10 spectroscopic sample, and should not be extrapolated out of this scope.

⁸ As a matter of comparison, Hildebrandt et al. (2010) used 14 distinct bands, while Abdalla et al. (2011) adopted all five SDSS bands.

⁹ A more robust statistical estimator against outliers are the median and median absolute deviation values (MAD). For this dataset, we obtained a median of 0.0048 and MAD = 0.0318.

4 Analytical photo-z determination

0.0302 and $0.0575 \leq \sigma_{(z_{\text{phot}} - z_{\text{spec}})} \leq 0.0973$. These values are compatible with those obtained by Eq. (1), $\langle z_{\text{phot}} - z_{\text{spec}} \rangle \approx 0.0104$, with a scatter¹⁰ of $\sigma_{(z_{\text{phot}} - z_{\text{spec}})} \approx 0.0570$. This reinforces the relevance of results achieved by the analytical expression derived with EUREQA. Despite its simple nature, it was able to deliver competitive accuracy and precision from a rather diverse and inhomogeneous sample.

We have also explicitly searched for expressions incorporating the u or z filters. One example of such functional form is

$$z_{\text{phot}} = 0.4583(r - i) + \frac{0.001i^2r - 0.3170r}{4.6691 + (u - i)(g - r)}. \quad (2)$$

Using this equation, we achieved accuracy and precision levels of $\langle (z_{\text{phot}} - z_{\text{spec}})/(1 + z_{\text{spec}}) \rangle \approx 0.0022$ and $\sigma_{(z_{\text{phot}} - z_{\text{spec}})/(1 + z_{\text{spec}})} \approx 0.0521$, respectively. These results are not better than those obtained with Eq 1, exemplifying that a larger number of filters does not necessarily lead to a more accurate photometric redshift estimation.

To estimate the level of bias introduced by Eq. (1) into a given cosmological inference, it is necessary to discuss the number of catastrophic errors, i.e., cases when photo-z is above a given tolerance threshold (Bernstein & Huterer 2010). These authors consider catastrophic errors as $|z_{\text{phot}} - z_{\text{spec}}| \gtrsim 1$, while Hildebrandt et al. (2010) defined them as $|z_{\text{phot}} - z_{\text{spec}}| > 0.15(1 + z_{\text{spec}})$ or > 0.5 . Molino et al. (2013) consider redshift dependent limits in terms of median and MAD, which in our context means $|z_{\text{phot}} - z_{\text{spec}}| \geq 0.2$ at $z = 0$ and 0.39 at $z = 1.0$. Figure 3 shows the catastrophic error rate obtained from Eq. (1) as a function of z_{spec} for three different scenarios: $|z_{\text{phot}} - z_{\text{spec}}| > 0.1, 0.25$ and 0.5 . The choice of three independent criteria gives a glimpse of how Eq. (1) performs in a wide range of accuracy requirements. In each panel the barplots are given in logarithm scale, where face-down bars indicate less than one percent of catastrophic errors according to the criteria on the right.

5 CONCLUSIONS

This work is the first attempt to use a heuristic machine assistant to propose new analytical relationships for photo-z estimation. It provides a simple and accurate functional form based on photometric information of SDSS spectroscopic sample galaxies. Although we started the search using all five SDSS bands, several solutions relied only on three of them. Hence, showing that for SDSS bands, a competitive performance can be attained even with a moderate number of filters.

We adopted a set of 41,214 galaxies for determining the photo-z expression. Afterwards, it was used to estimate z_{phot} for another 1,417,181 galaxies with known z_{spec} . Our results achieved $\langle (z_{\text{phot}} - z_{\text{spec}})/(1 + z_{\text{spec}}) \rangle \lesssim 0.0086$ and a scatter $\sigma_{(z_{\text{phot}} - z_{\text{spec}})/(1 + z_{\text{spec}})} \lesssim 0.045$ when averaged up to $z \lesssim 1.0$. These results indicate that symbolic regression is competitive against other methods available in the literature. An inspection of the $(z_{\text{phot}} - z_{\text{spec}})/(1 + z_{\text{spec}})$ distributions per redshift bin reveals systematic effects at $z_{\text{spec}} \gtrsim 0.7$. Such behavior might be caused by the poor statistics at high redshifts.

The conciseness of the outcomes obtained by EUREQA are stressed by how easily they can be adopted by the astronomical

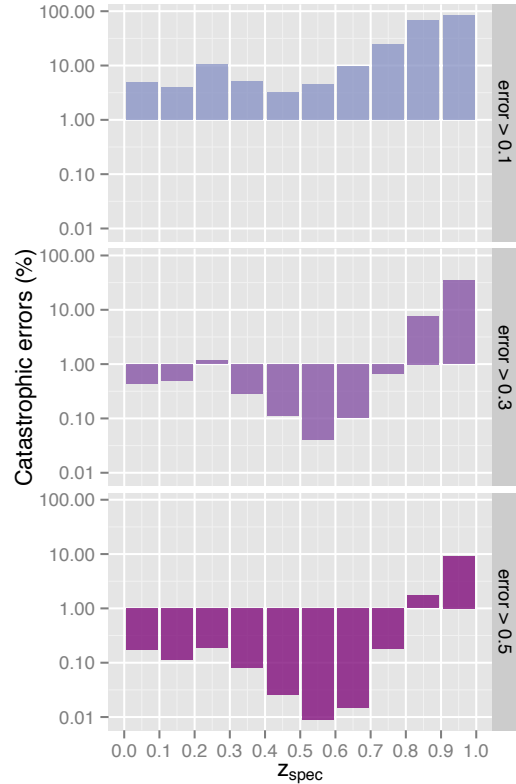


Figure 3. Percentual of catastrophic errors resulting from the photo-z estimation at each redshift bin for three different scenarios: $|z_{\text{phot}} - z_{\text{spec}}| > 0.1, 0.3$ and 0.5 , from top to bottom.

community. The functions can even be directly incorporated into simple SQL queries. Such level of portability is unattainable by the majority of photo-z methods currently available (but see e.g. Connolly et al. 1995; Hsieh et al. 2005). Moreover, the error propagation can be straightforwardly achieved by deriving the redshift as a function of photometric observables (e.g., Collister & Lahav 2004; Oyaizu et al. 2008).

Finally, the possibility to use computers to unveil hidden analytical relationships in datasets, a heretofore task exclusive of humans, is astonishing (e.g. Schmidt & Lipson 2009; Graham et al. 2013). Astronomy is already being flooded by an unprecedented amount of data, and this tendency is expected to increase even more in the next decade. Therefore the possibility to connect these novel systems to databases, and particularly allowing them to perform text mining in scientific literature (as in Leach et al. 2009), might represent a new paradigm for astronomical exploration. These methods are coming to stay, and although still incipient and naive, they host a great potential to help humankind in its endeavour to unravel the Universe.

ACKNOWLEDGMENTS

We thank Reinaldo Ramos de Carvalho, Andressa Jendrieck, Laerte Sodré Jr., Filipe Abdalla, Jon Loveday, Matias Carrasco, Jonatan D. Hernandez Fernandez and Ana Laura O’Mill for interesting suggestions and comments. EEOI and RSS thank the SIM Laboratory of the *Universidade de Lisboa* for hospitality during the development of this work. This work was partially supported

¹⁰ Using robust statistics, we obtain a median of 0.0062 and MAD = 0.0414.

by the ESA VA4D project (AO 1-6740/11/F/MOS). AKM thanks the Portuguese agency *Fundação para Ciência e Tecnologia, FCT*, for financial support (SFRH/BPD/74697/2010). EEOI thanks the Brazilian agencies FAPESP (2011/09525-3) and CAPES (9229-13-2) for financial support. Funding for SDSS-III has been provided by the Alfred P. Sloan Foundation, the Participating Institutions, the National Science Foundation, and the U.S. Department of Energy Office of Science. The SDSS-III web site is <http://www.sdss3.org/>. This work was written on the collaborative ShareLaTeX platform.

APPENDIX A: COMPARISON WITH OTHER METHODS

To compare symbolic regression with other methods and better situate our results, we adopted a publicly available data set that was previously submitted to different photo- z codes. The *PHoto-z Accuracy Testing* (PHAT) was an international initiative to identify the most promising photo- z methods and guide future improvements. Two observational photometric catalogues were provided: PHAT0 with simulations, and PHAT1 with real observations. A total of 17 photo- z codes were submitted. As a direct comparison using PHAT1 is not possible, as the answers of the challenge are not openly available, we applied symbolic regression to PHAT0 and compare its results to those reported by Hildebrandt et al. (2010).

We start by splitting the original dataset, comprised by 169520 simulated galaxies in two parts: one to derive the analytical photo- z expression, while another to assess the bias, scatter and outliers. For the former, in each redshift bin of $\Delta z = 0.1$ with more than 6000 objects, 3000 galaxies were randomly selected. In redshift bins with less than 6000 objects (e.g. higher redshift bins), half of the available galaxies were taken. The final subset comprises 29839 galaxies. The remaining ones were used to assess the expression estimates. As for the SDSS-DR10 sample, we considered only the basic mathematical blocks (+, -, *, /), resulting in:

$$z_{\text{phot}} = \frac{0.3375 + 0.3497(r - z) + 0.3924(u - g)(Y - K) - (Y - J)(Y - K) - 0.4465(u - g) + 0.61803(J - K) + 3.4495(Y - K)(Y - J)^2}{(u - i)}. \quad (\text{A1})$$

This expression, when applied to the validation data set yields $\langle (z_{\text{phot}} - z_{\text{spec}})/(1 + z_{\text{spec}}) \rangle = 0.001$, $\sigma_{(z_{\text{phot}} - z_{\text{spec}})/(1 + z_{\text{spec}})} = 0.039$ and an outlier fraction of 4.331%. Here we report the outlier fraction as $|z_{\text{phot}} - z_{\text{spec}}| > 0.15(1 + z_{\text{spec}})$, according to the definition adopted by Hildebrandt et al. (2010). Results for all 17 photo- z codes submitted to PHAT for the PHAT0 data set can be summarized as: $-0.05 \leq (z_{\text{phot}} - z_{\text{spec}})/(1 + z_{\text{spec}}) \leq 0.001$, $0.010 \leq \sigma_{(z_{\text{phot}} - z_{\text{spec}})/(1 + z_{\text{spec}})} \leq 0.049$ and outlier fraction between 0.010% and 18.202%. Comparing these results, we confirm that the accuracy of our results are within the values reported by other widely used methods.

Finally, Figure 4 shows the error distributions per redshift bin. Most of the data used to derive the expression ($\approx 99.5\%$) is concentrated at $z \leq 1.45$, which not surprisingly corresponds to the interval where the photo- z determination is more accurate. On the other hand, the expression shows a degraded performance at higher redshifts (which contain less than $\approx 0.5\%$ of the data). This is similar to the results found for the SDSS-DR10 sample, indicating that in cases where a homogeneous data distribution is available, the symbolic regression results are competitive to available methods.

REFERENCES

- Abdalla F. B., Banerji M., Lahav O., Rashkov V., 2011, *MNRAS*, 417, 1891
- Ahn C. P., Alexandroff R., Allende Prieto C., Anders F., Anderson S. F., Anderton T., Andrews B. H., Aubourg É., et. al 2013, arXiv:1307.7735
- Benítez N., 2000, *ApJ*, 536, 571
- Bernstein G., Huterer D., 2010, *MNRAS*, 401, 1399
- Bolzonella M., Miralles J.-M., Pelló R., 2000, *A&A*, 363, 476
- Carrasco Kind M., Brunner R. J., 2013, *MNRAS*, 432, 1483
- Collister A. A., Lahav O., 2004, *PASP*, 116, 345
- Connolly A. J., Csabai I., Szalay A. S., Koo D. C., Kron R. G., Munn J. A., 1995, *AJ*, 110, 2655
- de Simoni F., Sobreira F., Carnero A., Ross A. J., Camacho H. O., Rosenfeld R., Lima M., da Costa L. A. N., Maia M. A. G., 2013, *MNRAS*, 435, 3017
- Graham M. J., Djorgovski S. G., Mahabal A. A., Donalek C., Drake A. J., 2013, *MNRAS*, 431, 2371
- Green J., Schechter P., Baltay C., Bean R., Bennett D., Brown R., Conselice C., Donahue M., et al. 2012, arXiv:1208.4012
- Hildebrandt H., Arnouts S., Capak P., Moustakas L. A., Wolf C., Abdalla F. B., Assef R. J., Banerji M., et. al 2010, *A&A*, 523, A31
- Hsieh B. C., Yee H. K. C., Lin H., Gladders M. D., 2005, *ApJS*, 158, 161
- Ilbert O., Arnouts S., McCracken H. J., Bolzonella M., Bertin E., Le Fèvre O., Mellier Y., Zamorani G., et al. 2006, *A&A*, 457, 841
- Kessler R., Cinabro D., Bassett B., Dilday B., Frieman J. A., Garnavich P. M., Jha S., Marriner J., Nichol R. C., Sako M., Smith M., Bernstein J. P., Bizyaev D., Goobar A., Kuhlmann S., Schneider D. P., Stritzinger M., 2010, *ApJ*, 717, 40
- Koza J. R., 1992, *Genetic programming: on the programming of computers by means of natural selection*. MIT Press, Cambridge, MA, USA
- Leach S. M., Tipney H., Feng W., Baumgartner W. A., Kasliwal P., Schuyler R. P., Williams T., Spritz R. A., Hunter L., 2009, *PLoS Comput Biol*, 5, e1000215
- LSST Science Collaboration Abell P. A., Allison J., Anderson S. F., Andrew J. R., Angel J. R. P., Armus L., Arnett D., Asztalos S. J., Axelrod T. S., et al. 2009, arXiv:0912.0201
- Mandelbaum R., Seljak U., Hirata C. M., Bardelli S., Bolzonella M., Bongiorno A., Carollo M., Contini T., et al. 2008, *MNRAS*, 386, 781
- Miles N., Freitas A., Serjeant S., 2007, in Ellis R., Allen T., Tuson A., eds., *Applications and Innovations in Intelligent Systems XIV*. Springer London, pp 75–87
- Molino A., Benítez N., Moles M., Fernández-Soto A., Cristóbal-Hornillos D., Ascaso B., Jiménez-Teja Y., Schoenell W., et al. 2013, arXiv:1306.4968
- Nishizawa A. J., Oguri M., Takada M., 2013, *MNRAS*, 433, 730
- Nusser A., Branchini E., Feix M., 2013, *JCAP*, 1, 18
- O’Mill A. L., Duplancic F., García Lambas D., Sodré Jr. L., 2011, *MNRAS*, 413, 1395
- Oyaizu H., Lima M., Cunha C. E., Lin H., Frieman J., Sheldon E. S., 2008, *ApJ*, 674, 768
- Refregier A., Amara A., Kitching T. D., Rassat A., Scaramella R., Weller J., Euclid Imaging Consortium f. t., 2010, arXiv:1001.0061
- Reis R. R. R., Soares-Santos M., Annis J., Dodelson S., Hao J., Johnston D., Kubo J., Lin H., Seo H.-J., Simet M., 2012, *ApJ*, 747, 59
- Richards G. T., Myers A. D., Gray A. G., Riegel R. N., Nichol R. C., Brunner R. J., Szalay A. S., Schneider D. P., Anderson S. F., 2009, *ApJS*, 180, 67
- Schmidt M., Lipson H., 2009, *Science*, 324, 81
- Wadadekar Y., 2005, *PASP*, 117, 79
- Zheng H., Zhang Y., 2012, in *Society of Photo-Optical Instrumentation Engineers (SPIE) Conference Series Vol. 8451 of Society of Photo-Optical Instrumentation Engineers (SPIE) Conference Series, Review of techniques for photometric redshift estimation*
- Zitrin A., Broadhurst T., Coe D., Umetsu K., Postman M., Benítez N., Meneghetti M., Medezinski E., et. al 2011, *ApJ*, 742, 117

6 Analytical photo-z determination

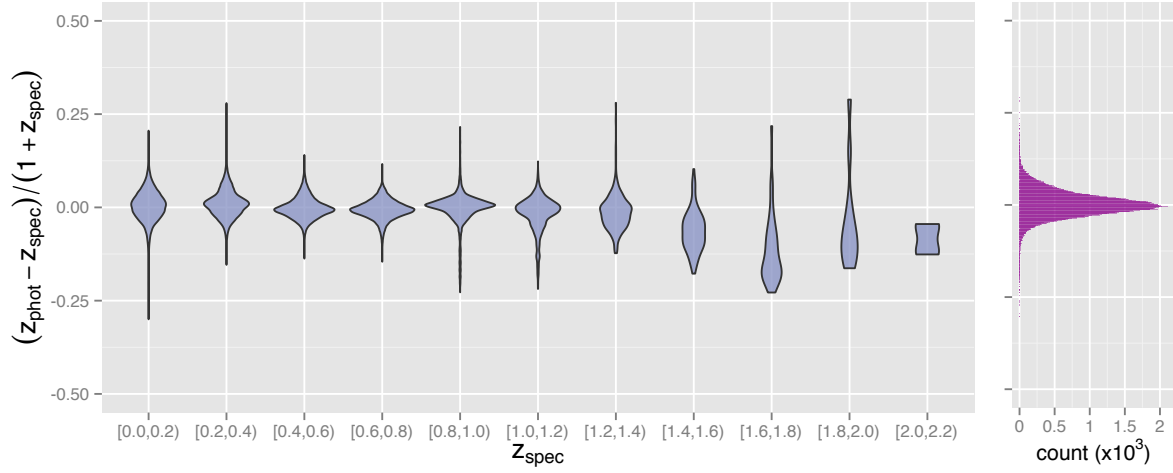


Figure 4. Left panel shows the photometric redshift error distributions for the PHAT0 dataset and equation (A1) in redshift bins of width $\Delta z_{\text{spec}} = 0.2$ in the range $[0 - 2.2)$. Right panel displays the error distribution all the galaxies (bins of width $\Delta((z_{\text{phot}} - z_{\text{spec}})/(1 + z_{\text{spec}})) = 0.001$).